Available online at www.sciencedirect.com
SCIENCE DIRECT
Bioorganic & Medicinal Chemistry Letters
Bioorganic & Medicinal Chemistry Letters 16 (2006) 1049–1053

A novel nicotinic acetylcholine receptor antagonist radioligand for PET studies

Yu-Shin Ding,[a,*] Kun-eek Kil,[a] Kuo-Shyan Lin,[b] Wei Ma,[c] Yasuno Yokota[c] and Ivy F. Carroll[c]

[a]*Chemistry Department, Brookhaven National Laboratory, Upton, NY 11973, USA*
[b]*Department of Radiology, University of Pittsburgh, Pittsburgh, PA 15213, USA*
[c]*Chemistry and Life Sciences, Research Triangle Institute, NC 27709, USA*

Received 18 September 2005; revised 18 October 2005; accepted 21 October 2005
Available online 11 November 2005

Abstract—Using positron emission tomography (PET) with a specific and selective radioligand targeting nicotinic acetylcholine receptor (nAChR) would allow us to better understand various nAChR related CNS disorders. The use of radiolabeled nAChR antagonists would provide a much safer pharmacological profile, avoiding most peripheral side effects that might be generated from radiolabeled nAChR agonists even at the tracer level; thus, PET imaging with nAChR antagonists would facilitate clinical application. A potent and selective nAChR antagonist was labeled and characterized with PET in non-human primates. Its high brain uptake, high signal-to-noise ratio, and high specific binding strongly suggest a great potential to carry out imaging studies in humans. In addition, the use of a C-11 radiotracer would allow us to perform multiple PET studies in the same individual within a short time frame. The presence of an iodine atom in the molecule also allows the possibility to label with radioiodine for SPECT studies.

Nicotine is one of the most abused reinforcing agents. Recent studies suggest that collectively, cardiovascular disease (including stroke), cancer, and diabetes account for approximately two-thirds of all deaths in the United States and the prevalence of tobacco use is one of the major risk factors for these diseases.[1] It is well documented that nicotinic acetylcholine receptors (nAChR) are the molecular target for nicotinic actions. Since nAChR plays a role in various neuropathological and physiological states, including Parkinson's disease (PD), Alzheimer's disease (AD), pain, tobacco dependency, schizophrenia, anxiety, and depression,[2–4] the ability to map this receptor, to measure the density, and to characterize abnormalities in various disease states is crucial. Using positron emission tomography (PET) and a specific and selective radioligand targeting nAChR would allow us to better understand these CNS disorders. In the past, most efforts have been directed toward the development of nAChR agonists,[5–9] and the use of radiolabeled nAChR agonists, such as 5-^{123}I-A-85380, 2-^{18}F-A-85380, and 6-^{18}F-A-85380, has proven possible for in vivo imaging in humans.[10–12] However, recent studies show that nAChR antagonists are effective in the treatment of smoking cessation.[13] In addition, the use of radiolabeled nAChR antagonists would provide a much safer pharmacological profile avoiding most peripheral side effects that might be generated from radiolabeled nAChR agonists even at the tracer level;[14] thus, PET imaging with nAChR antagonists would facilitate clinical application.

Recently, a series of epibatidine analogues has been developed.[15–17] Some of these analogues showed high affinity for nAChR; however, relative to epibatidine, they showed weak agonist activity in the mouse antinociception and body temperature tests. Importantly, all compounds were potent nAChR functional antagonists of nicotine's antinociceptive effects in the tail-flick procedure. The high affinity of the *N*-methyl-3′-iodo epibatidine analogue (NMI-EPB, 7-methyl-2-*exo*-(3′-iodo-5′-pyridinyl)-7-azabicyclo[2.2.1]-heptane) combined with its weak agonist and potent antagonist activity makes it one of the most promising ligands for this develop-

Keywords: nAChR; Antagonist; PET; C-11.
* Corresponding author. Tel.: +1 631 344 4388; fax: +1 631 344 5815; e-mail: ding@bnl.gov

0960-894X/$ - see front matter © 2005 Elsevier Ltd. All rights reserved.
doi:10.1016/j.bmcl.2005.10.075

ment work. In this paper, we describe the C-11 radiolabeling of NMI-EPB ([^{11}C]NMI-EPB) and its evaluation in baboons with PET.

[^{11}C]NMI-EPB was obtained using a procedure similar to that described in our previous papers for the radiosynthesis of norepinephrine ligands[18,19] by alkylating 1.0 mg of the corresponding demethylated precursor[16] of NMI-EPB in DMF (0.25 mL) with [^{11}C]methyl iodide. After 5 min at 110 °C, the product was purified by HPLC using a Phenomenex Luna C-18 semi-preparative column (250 mm × 10 mm, 5 μm) eluting with 20:80 CH_3CN/0.2 M NH_4OAc at a flow rate of 3.0 mL/min. After HPLC purification, [^{11}C]NMI-EPB was obtained in 40 ± 8% radiochemical yields (n = 22). The radiochemical purities were determined by an analytical radio-HPLC system and a TLC system in the presence of the unlabeled reference compound as a carrier. The total radiosynthesis time was 40 min with an average specific activity of 2–10 Ci/mol at the end of bombardment and the radiochemical purity >98%. The prepared radiotracers were immediately injected into baboons for PET studies and the average specific activity at the time of injection was ~0.5–2.5 Ci/μmol.

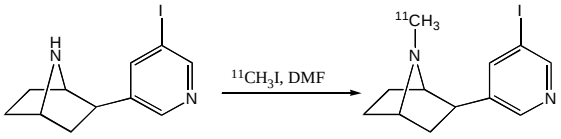

[^{11}C]NMI-EPB

We used dynamic PET scanning (Siemen's HR+ high resolution, whole body PET scanner with 4.5 × 4.5 × 4.8 mm at center of field of view) in 3-D mode for a period of 90 min combined with pharmacologic intervention to evaluate [^{11}C]NMI-EPB. Methodologies for scanning and image analysis in baboons generally follow the studies described in our recent publications for norepinephrine ligands,[20,21] Reproducibility of the tracer binding was demonstrated by a test/retest pair study on the same baboon on the same day with a 2 h interval between studies. The saturability and specificity of the tracer binding to nAChR were determined by carrying out blocking studies with unlabeled nicotine, and the tracer reversibility was characterized by displacement studies with either unlabeled nicotine or the unlabeled parent compound (NMI-EPB). All animal studies were conducted in strict accordance with the NIH Guide for the Care and Use of Laboratory Animals and approved by the BNL Animal Care Committee. Vital signs including heart rate, blood pressure, and respiration rate during all drug interventions were continuously monitored and showed no unusual deviation from the baseline values.

Plasma radioactivity and metabolite analysis. The percentage unchanged for the tracer in baboon plasma was assayed as described previously[20,21] via the HPLC and solid phase extraction methods. The results were similar for both methods, with 96%, 70%, 46%, and 26% as unchanged [^{11}C]NMI-EPB at 1, 5, 10, and 30 min. Only polar metabolites were found in baboon plasma following iv injection of the tracer.

Lipophilicity (log P) and plasma protein binding (PPB). Log P and PPB were determined according to the procedure described previously.[20,21] Log P was found to be 1.09. The free fraction in the plasma was 40%, based on the ratio of the decay-corrected counts of the unbound aliquots to the decay-corrected counts of the unspun aliquots.

Test/retest reproducibility. The regional distribution of the radioactivity after injection of [^{11}C]NMI-EPB in baboon brain is consistent with the known distribution of nAChR,[5,10] with the highest uptake occurring in the thalamus (TH, ~0.05% injected dose/cc, peaked at 3–5 min), intermediate in midbrain (MB) and brain stem, lower in cortical regions, and lowest in cerebellum (CB). The time–activity curves for various brain regions were very similar for test and retest studies (Fig. 1), indicating the reproducibility of tracer binding. The ratio for the radioactivity in TH to that in CB was greater than 3.0 at about 45 min after injection for this baboon, and the TH-to-CB ratio plateaued thereafter.

Blocking studies. Nicotine (0.03 mg/kg) was given intravenously at 5 min prior to tracer injection and the time–activity curves for TH, MB, and CB at baseline and after treatment with nicotine are shown in Figure 2A. The corresponding plots for the TH-to-CB ratio are shown in Figure 2B. Excellent blocking by nicotine was observed, demonstrating the specific binding of the tracer. This degree of blocking was also dose-dependent (data

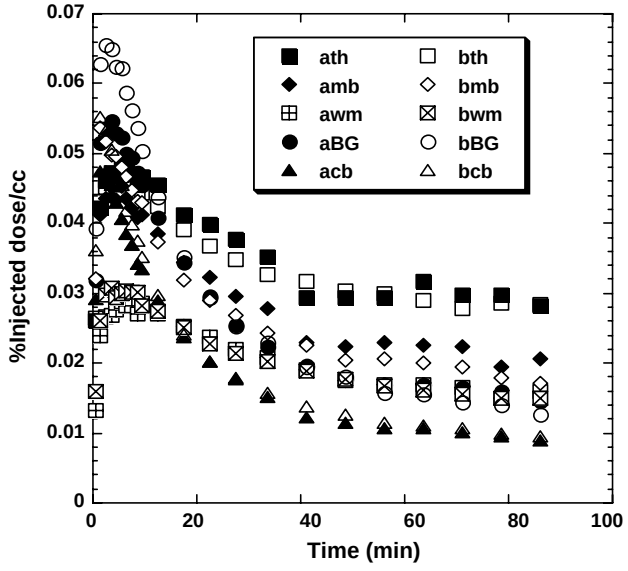

Figure 1. Test (a, solid symbols) and retest (b, open symbols) reproducibility after injection of [^{11}C]NMI-EPB in the same baboon with a 2 h interval between studies: time–activity curves in thalamus (squares), mid-brain (diamonds), white matter (squares with cross), basal ganglia (circles), and cerebellum (triangles).

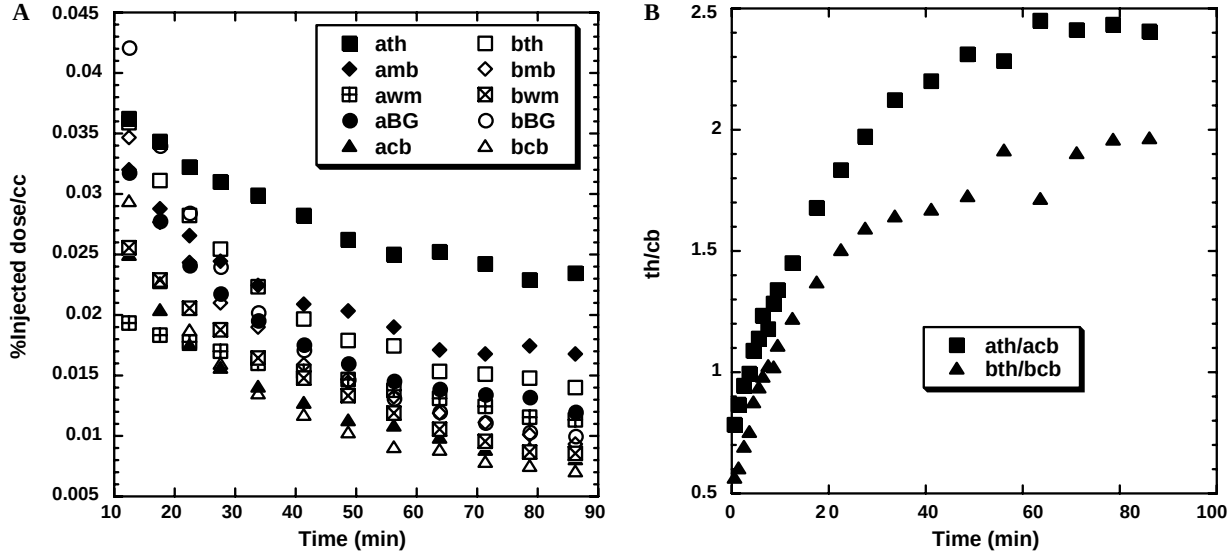

Figure 2. Blocking study: (A) time–activity curves for [^{11}C]NMI-EPB in thalamus (squares), mid-brain (diamonds), white matter (squares with cross), basal ganglia (circles), and cerebellum (triangles) before (a, solid symbols) and after (b, open symbols) nicotine pretreatment. Thalamus-to-cerebellum ratios are presented for the same data in (B).

not shown), indicating the saturability of the tracer binding to the nAChR.

Displacement studies. In a chase experiment, [^{11}C]NMI-EPB binding proved to be reversible as the injection of unlabeled either nicotine (0.03 mg/kg, Fig. 3A) or parent compound (unlabeled NMI-EPB, data not shown) at 20 min post to tracer injection induced a large displacement of thalamus activity to a level of the baseline striatal activity (the timing and dose for this displacement have not been optimized). As a result, the TH/CB ratio dropped from 3.7 to 1.9 at the end of the study (Fig. 3B). Corresponding PET images (summed images for entire frames) showed a significantly reduced binding in the displacement study as compared to the baseline.

Based on the pharmacological tests (tail-flick, hot plate, and body temperature), substitution at the 3′-pyridine position of a series of deschloroepibatidine analogues dramatically reduced agonist potency in all behavior measures as compared to epibatidine analogues. Among these analogues, *N*-methyl-3′-iodo epibatidine (NMI-EPB) displays high affinity toward α4β2 (K_i = 0.029 nM against [^{3}H]epibatidine) and potent functional antagonist property against nicotine-induced antinociception (AD_{50} = 0.04 μg/kg in the tail-flick test). These in vitro data appear to be more promising than a recent report for an F-18 labeled putative antagonist nifrolidine[22] (K_i = 2.89 nM against [^{125}I]iodoepibatidine). Although it has been shown that inclusion of alkyl groups (*n*-propyl and *n*-butyl) at the 3′-pyridine position in pyridylethers changes their agonist character to an antagonist character,[23] the antagonist properties of nifrolidine have not been confirmed yet.

Our PET studies of [^{11}C]NMI-EPB in baboon revealed its excellent ability to penetrate the blood–brain barrier and localize selectively in the brain regions that are consistent with the known concentrations of nAChR. The % injected dose/cc in the brain after injection of [^{11}C]NMI-EPB (~0.05%) was much higher than those obtained from 2-^{18}F-A-85380 and 6-^{18}F-A-85380 (less than 0.02% based on our comparative studies in baboon reported previously[9]), in spite of the fact that the log *P* values were 1.09 and 1.25 for [^{11}C]NMI-EPB and 6-^{18}F-A-85380, respectively. All of the radiolabeled plasma metabolites of [^{11}C]NMI-EPB are polar species and are not expected to enter the brain. The determination of the chemical form in the brain after tracer injection in mice is currently under investigation.[24–26] The reproducibility, specificity, saturability, and reversibility of [^{11}C]NMI-EPB were clearly shown via our characterization studies in baboon. Interestingly, the binding of [^{11}C]NMI-EPB in white matter (higher than cerebellum) was also observed, and the binding can be either blocked or displaced by nicotine when nicotine is injected either 5 min prior to or 20 min post tracer injection, as indicated in Figures 2A and 3A, respectively. These results were similar to those we presented in our previous studies in both baboons and humans,[12] suggesting that this tracer might also be a potential tool to probe the functional significance of nAChR in white matter. Most importantly, our studies demonstrate that [^{11}C]NMI-EPB exhibits relatively faster kinetics ($t_{1/2}$ = 60–90 min for clearance) and might possibly be able to achieve an equilibrium in vivo much faster than all of the existing radioligands, including 2-^{18}F-A-85380,[11,27] 6-^{18}F-A-85380,[12] and ^{18}F-nifrolidine.[22] Furthermore, the use of a C-11 radiotracer would allow us to carry out two to three scans on the same subject on the same day. Graphical analysis of the tracer binding is in progress, and its affinities toward different nAChR subtypes are currently under investigation.

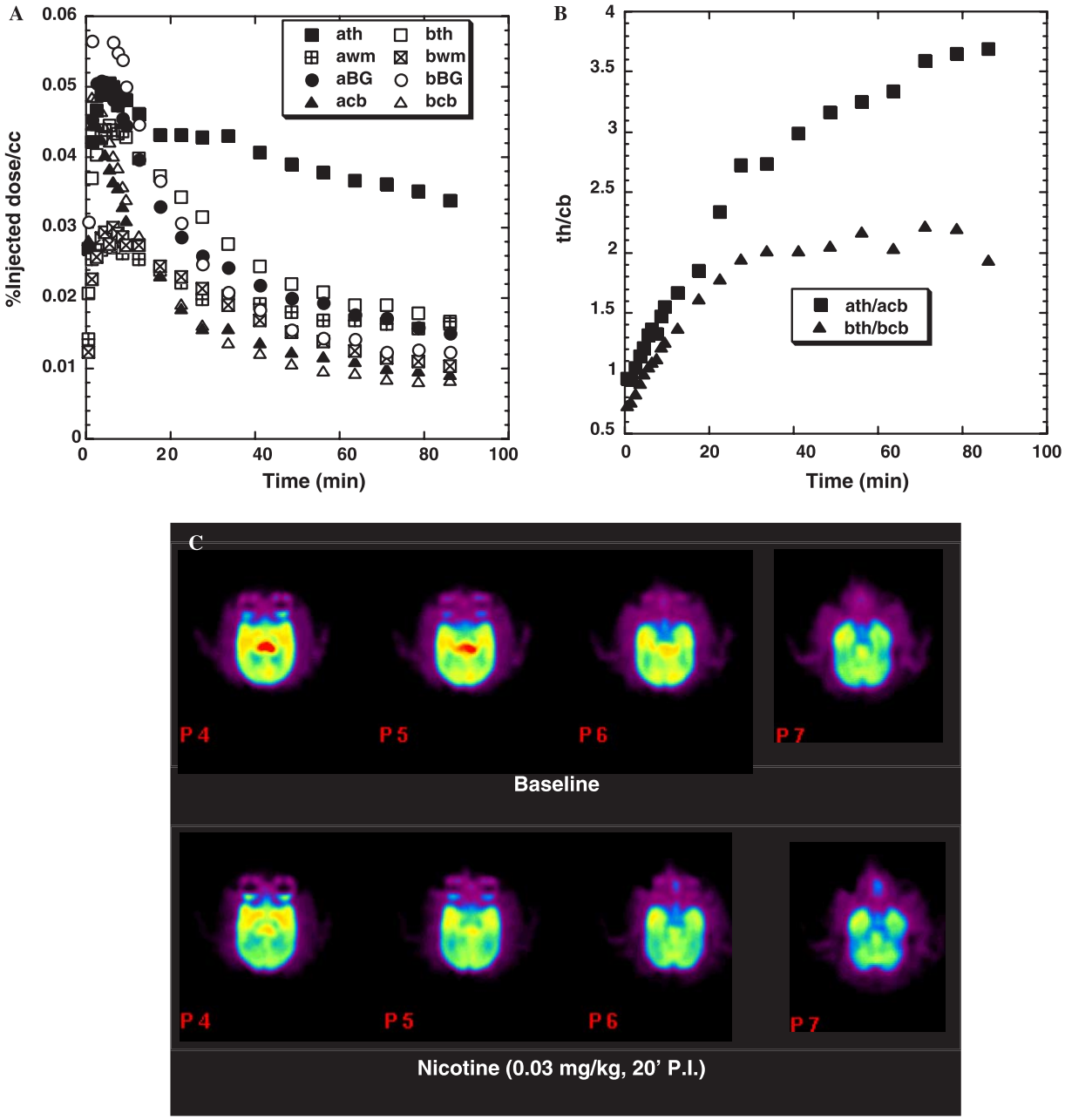

Figure 3. Displacement study: (A) time–activity curves for [^{11}C]NMI-EPB in thalamus (squares), white matter (squares with cross), basal ganglia (circles), and cerebellum (triangles) at baseline (a, solid symbols) and with nicotine injection at 20 min post tracer injection (b, open symbols). Thalamus-to-cerebellum ratios are presented for the same data in (B). Comparative PET images (summed images 0–90 min) are presented in (C).

Acknowledgments

This research was carried out at Brookhaven National Laboratory under contract DE-AC02-98CH10886 with the U.S. Department of Energy and Office of Biological Environmental Research and was also supported by the National Institutes of Health (EB002630, DA-06278, and DA 12001). The authors are grateful to P. Carter, P. King, D. Warner, C. Shea, Y. Xu, D. Alexoff, M. J. Schueller, D. J. Schlyer, R. A. Ferrieri, and J. S. Fowler for their assistance.

References and notes

1. Eyre, H.; Kahn, R.; Robertson, R. M.; Clark, N. G.; Doyle, C.; Gansler, T.; Glynn, T.; Hong, Y.; Smith, R. A.; Taubert, K.; Thun, M. J. *CA Cancer J. Clin.* **2004**, *54*, 190.
2. Domino, E. F. *Neuropsychopharmacology* **1998**, *18*, 456.
3. Peto, R.; Lopez, A. D.; Boreham, J.; Thun, M.; Heath, C. J.; Doll, R. *Br. Med. Bull.* **1996**, *52*, 12.
4. Pontieri, F. E.; Tanda, G.; Orzi, F.; Di Chiara, G. *Nature* **1996**, *382*, 255.

5. Ding, Y.-S.; Gatley, S. J.; Fowler, J. S.; Volkow, N. D.; Aggarwal, D.; Logan, J.; Dewey, S. L.; Liang, F.; Carroll, F. I.; Kuhar, M. J. *Synapse* **1996**, *24*, 403.
6. Ding, Y.-S.; Molina, P.; Fowler, J.; Logan, J.; Volkow, N.; Kuhar, M.; Carroll, F. *Nucl. Med. Biol.* **1999**, *26*, 139.
7. Ding, Y.-S.; Volkow, N. D.; Logan, J.; Garza, V.; Pappas, N.; King, P.; Fowler, J. S. *Synapse* **2000**, *35*, 234.
8. Ding, Y.-S.; Logan, J.; Bermel, R.; Garza, V.; Rice, O.; Fowler, J. S.; Volkow, N. D. *J. Neurochem.* **2000**, *74*, 1514.
9. Ding, Y.-S.; Liu, N.; Wang, T.; Marecek, J.; Garza, V.; Ojima, I.; Fowler, J. S. *Nucl. Med. Biol.* **2000**, *27*, 381.
10. Fujita, M.; Seibyl, J. P.; Vaupel, D. B.; Tamagnan, G.; Early, M.; Zoghbi, S. S.; Baldwin, R. M.; Horti, A. G.; Koren, A. O.; Mukhin, A. G.; Khan, S.; Bozkurt, A.; Kimes, A. S.; London, E. D.; Innis, R. B. *Eur. J. Nucl. Med. Mol. Imaging* **2002**, *29*, 183.
11. Kimes, A. S.; Horti, A. G.; London, E. D.; Chefer, S. I.; Contoreggi, C.; Ernst, M.; Friello, P.; Koren, A. O.; Kurian, V.; Matochik, J. A.; Pavlova, O.; Vaupel, D. B.; Mukhin, A. G. *FASEB J.* **2003**, *17*, 1331.
12. Ding, Y.-S.; Fowler, J. S.; Logan, J.; Wang, G.-J.; Telang, F.; Garza, V.; Biegon, A.; Pareto, D.; Rooney, W.; Shea, C.; Alexoff, D.; Volkow, N. D.; Vocci, F. *Synapse* **2004**, *53*, 184.
13. McRobbie, H. *Br. J. Cardiol.* **2005**, *12*, 37.
14. Molina, P. E.; Ding, Y.-S.; Carroll, F. I.; Liang, F.; Volkow, N. D.; Pappas, N.; Kuhar, M.; Abumrad, N.; Gatley, S. J.; Fowler, J. S. *Nucl. Med. Biol.* **1997**, *24*, 743.
15. Carroll, F. I.; Ware, R.; Brieaddy, L. E.; Navarro, H. A.; Damaj, M. I.; Martin, B. R. *J. Med. Chem.* **2004**, *47*, 4588.
16. Carroll, F. I.; Ma, W.; Yokota, Y.; Lee, J. R.; Brieaddy, L. E.; Navarro, H. A.; Damaj, M. I.; Martin, B. R. *J. Med. Chem.* **2005**, *48*, 1221.
17. Huang, Y.; Zhu, Z.; Xiao, Y.; Laruelle, M. E. *Bioorg. Med. Chem. Lett.* **2005**, *15*, 4385.
18. Lin, K.-S.; Ding, Y.-S. *Chirality* **2004**, *16*, 475.
19. Lin, K.-S.; Ding, Y.-S. *Bioorg. Med. Chem.* **2005**, *13*, 4658.
20. Ding, Y.-S.; Lin, K.-S.; Garza, V.; Carter, P.; Alexoff, D.; Logan, J.; Shea, C.; Xu, Y.; King, P. *Synapse* **2003**, *50*, 345.
21. Ding, Y.-S.; Lin, K. S.; Benveniste, H.; Carter, P. *J. Neurochem.* **2005**, *94*, 337.
22. Chattopadhyay, S.; Xue, B.; Collins, D.; Pichika, R.; Bagnera, R.; Leslie, F. M.; Christian, B. T.; Shi, B.; Narayanan, T. K.; Potkin, S. G.; Mukherjee, J. *J. Nucl. Med.* **2005**, *46*, 130.
23. Lin, N. H.; Gunn, D. E.; Li, Y.; He, Y.; Bai, H.; Ryther, K. B.; Kuntzweiler, T.; Donnelly-Roberts, D. L.; Anderson, D. J.; Campbell, J. E.; Sullivan, J. P.; Arneric, S. P.; Holladay, M. W. *Bioorg. Med. Chem. Lett.* **1998**, *8*, 249.
24. Ding, Y.-S.; Gatley, S. J.; Fowler, J. S.; Chen, R.; Volkow, N. D.; Logan, J.; Shea, C. E.; Sugano, Y.; Koomen, J. *Life Sci.* **1996**, *58*, 195.
25. Kiyono, Y.; Kanegawa, N.; Kawashima, H.; Kitamura, Y.; Iida, Y.; Saji, H. *Nucl. Med. Biol.* **2004**, *31*, 147.
26. Mathis, C. A.; Wang, Y.; Holt, D. P.; Huang, G.-F.; Debnath, M. L.; Klunk, W. E. *J. Med. Chem.* **2003**, *46*, 2740.
27. Chefer, S. I.; London, E. D.; Koren, A. O.; Pavlova, O. A.; Kurian, V.; Kimes, A. S.; Horti, A. G.; Mukhin, A. G. *Synapse* **2003**, *48*, 25.